

# Collective resonance modes of Josephson vortices in sandwiched stack of $\text{Bi}_2\text{Sr}_2\text{CaCu}_2\text{O}_{8+x}$ intrinsic Josephson junctions

Myung-Ho Bae and Hu-Jong Lee

Department of Physics, Pohang University of Science and Technology, Pohang 790-784, Republic of Korea

(Dated: November 20, 2018)

We observed splitting of the low-bias vortex-flow branch in a dense-Josephson-vortex state into multiple sub-branches in current-voltage characteristics of intrinsic Josephson junctions (IJJs) of  $\text{Bi}_2\text{Sr}_2\text{CaCu}_2\text{O}_{8+x}$  single crystals in the long-junction limit. Each sub-branch corresponds to a plasma mode in serially coupled Josephson junctions. Splitting into low-bias linear sub-branches with a spread in the slopes and the inter-sub-branch mode-switching character are in good quantitative agreement with the prediction of the weak but finite inter-junction capacitive-coupling model incorporated with the inductive coupling. This suggests the importance of the role of the capacitive coupling in accurately describing the vortex dynamics in serially stacked IJJs.

PACS numbers: 74.72.Hs, 74.50.+r, 74.78.Fk, 85.25.Cp

Ever since the Josephson coupling was known to be established in  $\text{Bi}_2\text{Sr}_2\text{CaCu}_2\text{O}_{8+x}$  (Bi-2212) single crystals along the adjacent superconducting  $\text{CuO}_2$  bilayers much research interest has been focused on the dynamics of Josephson vortices in these intrinsic Josephson junctions (IJJs) in the long junction limit [1, 2, 3]. The interest stems mainly from that the Josephson vortex motion in stacked IJJs provides an ideal model to study the coupled nonlinear dynamic phenomena and also provides unique possibilities of applying stacked IJJs to high-frequency active devices such as sub-millimeter oscillators and mixers.

In Bi-2212 IJJs, superconducting  $\text{CuO}_2$  bilayers are much thinner than the  $c$ -axis London penetration depth,  $\lambda_{ab}$  ( $\sim 200$  nm) [4]. Then, in a transverse magnetic field, screening supercurrents are induced in the stacked superconducting layers, which give rise to the inductive coupling between adjacent IJJs [5]. This coupling is strong enough that it leads to mutual phase locking of Josephson vortex motion along the  $c$  axis of stacked junctions. It has been predicted that inductively coupled and thus collectively moving vortices may resonate with the plasma oscillation modes and induce sub-branch splitting of current-voltage ( $IV$ ) curves *near the bias voltages corresponding to plasma mode velocities*, which was confirmed by previous numerical analysis and observations [6]. This phase-locked coherence of the plasma oscillation may be exploited to develop sub-millimeter oscillator devices.

On the other hand, the thickness of  $\text{CuO}_2$  bilayers is comparable to the Debye charge screening length  $D$  so that the local charge neutrality in the bilayers breaks down [7]. This nonequilibrium charge variation in superconducting bilayers yields adjacent IJJs are capacitively coupled as well. The purely capacitive coupling effect was treated theoretically before [8]. Recently, a model of the capacitive coupling incorporated with the strong inductive coupling has been proposed, where the capacitive coupling is taken into account on an equal footing as the inductive one [9]. In spite of the relative weakness, the capacitive coupling is predicted to lead to sig-

nificant changes in the collective vortex dynamics. The model predicts an  $IV$  curve splits into linear multiple sub-branches with varied slopes, which corresponds to different plasma modes, *in the low-bias region of the collective Josephson vortex flow*. The spread of the sub-branch slopes is governed by the strength of the capacitive coupling, represented by a parameter  $\alpha [= \epsilon D^2 / (st)$ ;  $\epsilon$  is the dielectric constant of the insulating layer,  $s$  ( $= 0.3$  nm) and  $t$  ( $= 1.2$  nm) are the thickness of the superconducting and the insulating layers, respectively], which provides a convenient means to determine the strength of the capacitive coupling in IJJs.

The dynamics of Josephson vortices in stacked IJJs is known to be sensitive to the vortex density in the junctions [10]. The collective resonance is usually revealed in a high field range of  $H \gtrsim H_d [= \phi_0 / 2(s+t)\lambda_J]$ ;  $\phi_0$  is the flux quantum and  $\lambda_J$  is the Josephson penetration depth]. In this dense-vortex state the non-Josephson-like emission [11] and the Shapiro resonance steps [12] have been observed, confirming the coherence of the Josephson-vortex-lattice motion over the whole stacked IJJs. Especially, for a higher field range of  $H \gtrsim H_{hd}$  ( $= \phi_0 / (s+t)\lambda_J$ ), the transverse inter-vortex spacing becomes close to  $\lambda_J$  [13]. In this range the Josephson current along the length of a junction distributes almost sinusoidally so that the collective resonance is expected to be stronger. Little experimental studies, however, have been done for the collective motion in this highly dense-vortex region.

In this study, we investigated details of multiple plasma modes manifested in the Josephson vortex-flow branch (JVFB) of stacks of IJJs in a high magnetic field above  $H_d$ . In all the three samples examined sub-branch splitting was seen to start occurring for a field exceeding  $H_d$ . Especially, in the JVFB for a field above  $H_{hd}$ , we obtained clear hysteretic multiple sub-branches and mode switching between them. The linear sub-branches for different collective vortex modes exhibited a spread in the slopes. The values of the capacitive coupling parameter  $\alpha$ , estimated from the spread, for the three samples under study were within the range of the theoretical pre-

TABLE I: Sample parameters.  $N$  is the total number of IJJs,  $J_c$  the critical tunneling current,  $\beta_c [= (4I_c/\pi I_r)^2]$  the McCumber parameter,  $\lambda_J$  the Josephson penetration depth, and  $\alpha$  the capacitive-coupling parameter.

Sample number	stack size ( $\mu\text{m}^2$ )	$N$	$J_c$ ( $\text{A}/\text{cm}^2$ )	$\beta_c$	$\lambda_J$ ( $\mu\text{m}$ )	$\alpha$
SS1	$17 \times 1.5$	55	1000	2000	0.31	0.35
SS2	$16 \times 1.5$	25	1500	1300	0.25	0.17
SS3	$16 \times 1.4$	60	1270	2200	0.27	0.24

diction of the hybrid-coupling model [9]. In addition, mode velocities estimated from the inter-branch switching voltages were in reasonable quantitative agreement with the prediction of the model.

Slightly overdoped Bi-2212 single crystals used in this study were grown by the solid-state-reaction method [14]. Samples were micropatterned on the crystals into the geometry of a stack of junctions sandwiched between top (400 nm thick) and bottom (100 nm thick) Au electrodes [see the inset of Fig. 1(a)]. The sizes of the three stacks were  $17 \times 1.5 \mu\text{m}^2$  (SS1),  $16 \times 1.5 \mu\text{m}^2$  (SS2), and  $16 \times 1.4 \mu\text{m}^2$  (SS3). Since each superconducting bilayer in a stack of IJJs is much thinner than  $\lambda_{ab}$ , Josephson vortices in a usual mesa structure [15] are supposed to be strongly coupled to those in the basal stack underneath the mesa, which may significantly distort the dynamics of the Josephson vortices in the mesa itself. In this study the basal stack was removed by using the double-side-cleaving technique [16] to overcome this problem. The detailed sample fabrication process is described elsewhere [17]. Eliminating the basal part turned out to be essential to obtain ideal vortex-flow characteristics of stacked IJJs. This sandwiched-stack geometry allowed to examine the collective vortex dynamics over the whole thickness of a stack. The magnetic field was aligned in parallel with the plane of junctions within the resolution of 0.01 degree to minimize the pinning of Josephson vortices by the formation of pancake vortices in  $\text{CuO}_2$  bilayers [18]. All the measurements were done at 4.2 K in a two-terminal configuration [Fig. 1(a)]. The combined contact resistance for bottom and top interfaces ( $\sim 2 \text{ k}\Omega$  for SS1 and SS2, and  $\sim 600 \Omega$  for SS3) was subtracted numerically.

The sample parameters are listed in Table I. The number of IJJs in a sandwiched stack,  $N$ , was estimated from the number of zero-field quasiparticle curves (not shown). The McCumber parameter  $\beta_c$  was obtained from the zero-field return current  $I_r$  [as denoted by arrows in Fig. 1(a) for decreasing bias]. Fig. 1 shows the JVFB of sample SS1 with a single up-down bias sweep. The values of  $H_d$  and  $H_{hd}$  for SS1 estimated with  $\lambda_J$  were 2.2 and 4.4 T, respectively. Thus, the data in Figs. 1(a) and 1(b) correspond approximately to the two dense-vortex ranges,  $H \sim H_d$  and  $H \sim H_{hd}$ , respectively. The average slope,  $\Delta V/\Delta I$ , of the JVFB keeps increasing in proportion with the magnetic field intensity. A few voltage jumps are seen in the JVFB for fields beyond  $\sim 2.6 \text{ T}$  in the bias range

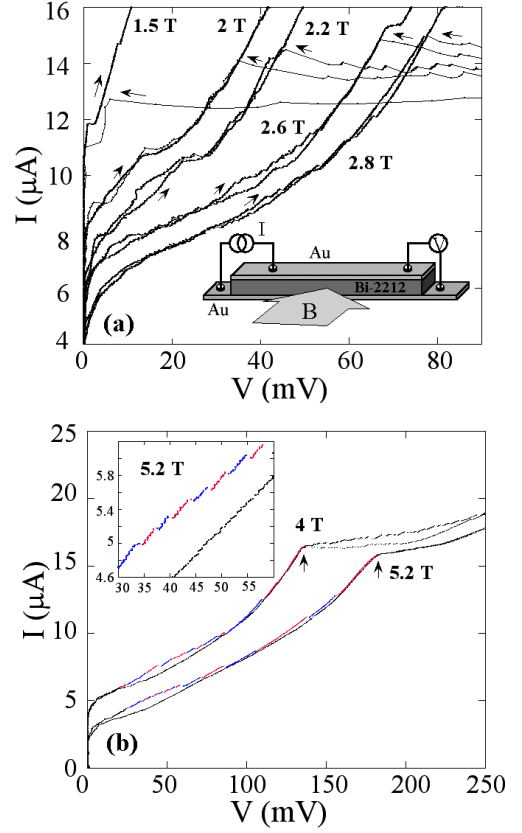


FIG. 1: (color). Josephson vortex-flow branches of SS1 in field ranges of (a)  $H \sim H_d$  and (b)  $H \sim H_{hd}$  (the 4-T curve is shifted upward by  $1 \mu\text{A}$ ). Neighboring sub-branches are colored alternately for clarity. The arrows in (a) indicate the current sweep direction. The arrows in (b) indicate the boundaries between the vortex-flow and the quasiparticle regions, defining the parameter  $V_c^{vf}$ . Inset of (a): the measurement configuration. Inset of (b): low-bias vortex-flow region at 5.2 T

above  $\sim 40 \text{ mV}$ . This unusual feature, taking place in the vortex-flow state for a bias below the quasiparticle-state return current  $I_r$  in each field, is caused by switching of coherent vortex-lattice motion between different plasma modes. Coherently moving vortex lattice remains in a certain transverse plasma mode as long as the vortex-lattice velocity is smaller than the propagation mode velocity of the plasma oscillation. Exceeding the mode velocity for a higher bias current, however, the resonating dynamic state of the Josephson vortex lattice suddenly switches to the adjacent plasma mode with a higher propagation velocity, giving rise to a voltage jump observed. The onset field of the observed voltage jumps almost coincides with the value of  $H_d$ .

Clearer voltage jumps in the JVFB are seen for a higher vortex density in the field range of  $H \gtrsim H_{hd}$  as in Fig. 1(b), as the resonant coupling between the vortex-lattice motion and the plasma oscillation is strengthened. In this field range the hysteresis in the quasi-particle branches

for  $V > V_c^{vf}$  (denoted by the arrows) in Fig. 1(b) is almost completely suppressed while the voltage jumps become more evident in JVFB. The inset of Fig. 1(b) shows the distinct voltage jumps in the lower bias region for 5.2 T. One notes that, in Fig. 1(b), all the voltage jumps take place in the low-bias flux-flow region bounded by  $V_c^{vf}$ . The voltage interval between the neighboring jumps tends to increase for higher biases, which is consistent with the prediction of both the purely inductive and the inductive-capacitive hybrid coupling models.

Fig. 2(a) displays the JVFB of the sample SS2 (with  $N=25$ ) taken for  $H=5.8$  T. For the measurement the bias current was repeatedly swept up and down so that detailed hysteretic feature of the sub-branches were traced out. These multiple-sweep data clearly indicate that the voltage jumps observed in the single-sweep data as seen in Fig. 1(b) were indeed caused by the inter-sub-branch mode switching. Since the  $H_{hd}$  for this sample is 5.4 T the data in Fig. 2 correspond to the highly dense vortex state of  $H \gtrsim H_{hd}$ , expectedly with many resonant vortex states as in the sample SS1 in the similar field range. About 22 multiple sub-branches were obtained in SS2, which was close to the number of the IJJs  $N=25$  in the stack. Details of the vortex-flow region of 5.2 T curve of SS1, as shown in Fig. 1(b), are also illustrated in Fig. 2(b) for a quantitative analysis.

In Figs. 2(a) and 2(b), all the discernible sub-branches exhibit linear  $IV$  characteristics in the low-bias vortex-flow region for  $V < V_c^{vf}$ , the occurrence of which is in agreement with the prediction of the inductive-and-capacitive hybrid coupling model. By contrast, the purely inductive coupling yields sub-branch splitting near the voltages corresponding to the plasma mode velocities. As denoted by the grey region in Fig. 2 the linear sub-branches, when extrapolated to the low-bias region, converges to a single intercept point with a positive value  $I_p$  on the current axis. It confirms the vortex-flow nature of the sub-branches with finite vortex pinning, that may have been caused by any defects in the IJJs or by any pancake vortices formed in  $\text{CuO}_2$  layers by a misaligned field component. The pinning current  $I_p$  was 2.07  $\mu\text{A}$  and 0.64  $\mu\text{A}$  in SS1 and SS2, respectively. For an analysis of the finite spread in the slopes of the linear sub-branches we adopt fitting to the hybrid coupling model [9], while incorporating the effect of the finite vortex pinning (represented by  $I_p$ ) and the change of the vortex density with applied magnetic fields ( $H_{ext}$ ) as

$$V = N(I - I_p) \left[ \frac{R_n}{A_n} + \frac{kH_{ext}}{I_c} \right]. \quad (1)$$

Here,  $A_n = 1 + 2\alpha[1 - \cos(n\pi/(N+1))]$ ,  $I_c$  is the critical Josephson current at a given applied field, and  $k$  is a constant. Since samples are in the quasiparticle state for  $V > V_c^{vf}$  we define the current corresponding to  $V_c^{vf}$  in a given field as the critical current  $I_c$  in Eq. (1). Also, the vortex velocity for  $I > I_p$  is assumed to increase linearly with the bias current.

Without the capacitive-coupling effect ( $\alpha=0$ ) the low-

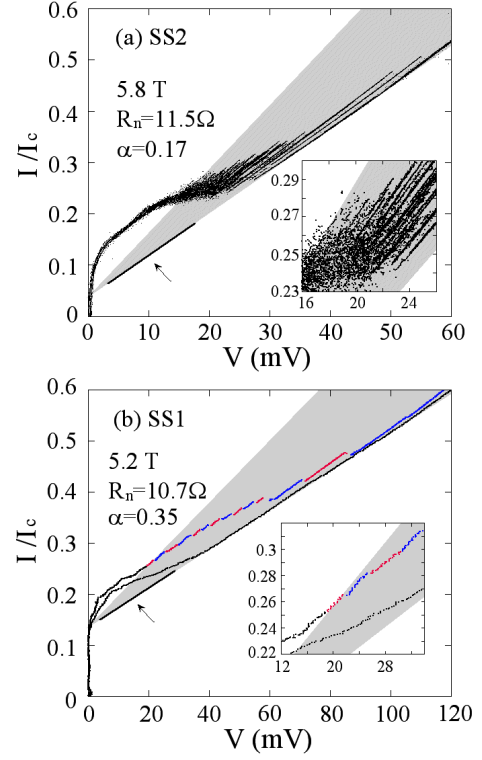


FIG. 2: (color). Josephson vortex-flow sub-branches (a) for SS2 at 5.8 T and (b) for SS1 at 5.2 T with the spread of linear sub-branches denoted by the gray region. Insets: details of the sub-branches in the low-bias range.

bias sub-branches with spreaded slopes, as exhibited by the grey regions in Figs. 2(a) and 2(b) for SS1 and SS2, respectively, are supposed to reduce to single lines (pointed by arrows), where the value of  $k$  determines the slope of the lines. Increasing  $\alpha$  the spread of sub-branch slopes increases from the  $\alpha=0$  lines to the left. In the very low bias region the JVFB in both samples becomes chaotic.

The parameter  $\alpha$  was determined from the best fit of the spread to Eq. (1), where the normal-state resistance  $R_n$  was fixed separately following the fitting procedure in Ref. [19]. The best-fit values of  $\alpha$  for SS1 at 5.2 T, SS2 at 5.8 T, and SS3 at 4.15 T were 0.35, 0.17, and 0.24, respectively. These values are in the range of theoretical estimate of the hybrid coupling model [9],  $0.1 \sim 0.4$ , and in reasonable agreement with the recently observed values of  $0.36 \sim 0.44$  in  $\text{SmLa}_{1-x}\text{Sr}_x\text{CuO}_{4-\delta}$  [20]. The corresponding values of the  $k$  for SS1, SS2, and SS3 were 0.32, 0.14, and 0.38 mV/T, respectively.

Fig. 3 displays the mode-switching voltages (filled circles) and boundary voltage  $V_c^{vf}$  (filled square) for SS2 as a function of the mode index  $n$ . Out of 25 expected modes corresponding to  $N$  the three lowest-index modes were not observed, however, presumably because they were located beyond  $V_c^{vf}$ . The solid line is the trace calculated with  $\alpha=0.17$  and the best fit value for the

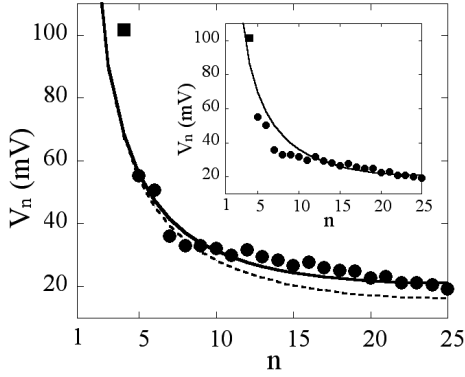


FIG. 3: Mode-switching voltages (filled circles) and  $V_c^{vf}$  (filled square) as a function of mode index  $n$  for SS2. The solid line is the best fit to the hybrid coupling model. The dotted line is obtained for the inductive coupling only, with the same parameters as used for the solid line. Inset: the best fit to the purely inductive coupling model.

Swihart velocity  $c_0 = 1.05 \times 10^5$  m/s. The resonance voltage of the  $n$ th mode is obtained from the relation [11]  $V_n = N c_n H_{ext}(t + s)$ . The mode velocity of the transverse plasma oscillation ( $c_n$ ) is expected to be enhanced by a factor of  $\sqrt{A_n}$  from that ( $c_n^0$ ) of the purely inductive coupling model ( $A_n = 1$ ) by the nonvanishing capacitive-coupling effect [9] as in the relation

$$c_n = c_0 \sqrt{\frac{A_n}{1 - \cos(\pi n / (N + 1))}} = c_n^0 \sqrt{A_n}, \quad (2)$$

where the mode index  $n$  runs from 1 to  $N$ . The dotted line corresponds to the case of purely inductive coupling ( $\alpha = 0$ ) with the same Swihart velocity as used for the solid line. One sees that the enhancement of the mode velocities due to nonvanishing capacitive coupling becomes more evident for high mode indices, giving a maximum enhancement for  $c_N$  as  $c_N = c_N^0 [(1 + 4\alpha)]^{1/2}$ . The inset of

Fig. 3 illustrates the best fit of the mode voltages to the purely inductive-coupling model, with the best-fit value of  $c_0$  to be  $1.35 \times 10^5$  m/s. In this case, mode voltages for low-index modes are seen to fall significantly below the model expectation. This trend was also observed previously in the motion of microwave-induced Josephson vortices, although the vortex density was much lower than in this study [15].

The Swihart velocity for SS2, estimated using the resistively shunted junction model, was  $c_0 = 2\pi f \lambda_J = 8.7 \times 10^4$  m/s. In the calculation we used the Josephson plasma frequency  $f_{pl}$  ( $= \sqrt{I_c / 2\pi \Phi_0 C_J}$ ) of 55 GHz, estimated from the critical current  $I_c = 0.358$  mA and the junction capacitance  $C_J = 9$  pF determined from  $\beta_c$  and  $R_n$ . The value of  $c_0$  is close to the one obtained for the hybrid-coupling model but tends to deviate more from the predication of the inductive-coupling model.

In summary, the observed characteristics of the sub-branch splitting in the vortex-flow region were in reasonable quantitative agreement with the inductive coupling incorporated with the capacitive coupling. The multiple sub-branches in JVFB were shown to be caused by the inter-junction capacitive coupling and the value of the coupling parameter  $\alpha$  estimated from the spread of multiple branches was in good agreement with the theoretical prediction of the hybrid coupling as well as the previous observation in optical measurement [20]. The quantitative identification of the multiple sub-branches in this study confirmed the significance of the capacitive coupling in addition to the inductive coupling in accurately describing the dynamics of Josephson vortices in serially stacked IJJs. For further detailed analysis of the Josephson vortex dynamics consideration of the charge-hole imbalance coupling [21] and the dissipation effect of quasiparticles in the  $ab$  plane [22] may be required.

We thank Ju H. Kim for valuable discussions. This work was supported by the National Research Laboratory project administrated by KISTEP.

- 
- [1] R. Kleiner *et al.*, Phys. Rev. Lett. **68**, 2394 (1992); A. Yurgens *et al.*, Phys. Rev. B **53**, R8887 (1994).
  - [2] S. Sakai *et al.*, J. Appl. Phys **73**, 2411 (1993); R. Kleiner, Phys. Rev. B. **50**, 6919 (1994); M. Machida *et al.*, Physica (Amsterdam) **330C**, 85 (2000).
  - [3] J. U. Lee *et al.*, Appl. Phys. Lett. **67**, 1471 (1995); V. M. Krasnov *et al.*, Phys. Rev. B **61**, 766 (2000).
  - [4] O. Waldmann *et al.*, Phys. Rev. B **53**, 11825 (1996).
  - [5] J. R. Clem and M. W. Coffey, Phys. Rev. B **42**, 6209 (1990).
  - [6] R. Kleiner *et al.*, Phys. Rev. B. **50**, 3942 (1994); A. Irie *et al.*, Appl. Phys. Lett. **72**, 2159 (1998); R. Kleiner *et al.*, Physica (Amsterdam) **362C**, 29 (2000).
  - [7] M. Machida *et al.*, Phys. Rev. Lett. **83**, 4618 (1999).
  - [8] T. Koyama and M. Tachiki, Phys. Rev. B. **54**, 16183 (1996);
  - [9] J. H. Kim, Phys. Rev. B **65**, 100509 (2002); J. H. Kim and J. Pokharel, Physica C **384**, 425 (2003).
  - [10] A. E. Koshelev, Phys. Rev. B **66**, 224514 (2002).
  - [11] G. Hechtfisher *et al.*, Phys. Rev. Lett. **79**, 1365 (1997).
  - [12] Yu. I. Latyshev *et al.*, Phys. Rev. Lett. **87**, 247007 (2001).
  - [13] L. Bulaevskii and J. R. Clem, Phys. Rev. B **44**, 10234 (1991).
  - [14] N. Kim *et al.*, Phys. Rev. B. **59**, 14639 (1999).
  - [15] Y.-J. Doh *et al.*, Phys. Rev. B. **63**, 144523 (2001).
  - [16] H. B. Wang *et al.*, Phys. Rev. Lett. **87**, 107002 (2001).
  - [17] M. H. Bae *et al.*, Appl. Phys. Lett. **83**, 2187 (2003).
  - [18] G. Hechtfisher *et al.*, Phys. Rev. B **55**, 14638 (1997); A. Irie *et al.*, Phys. Rev. B **62**, 6681 (2000).
  - [19] H. Won and K. Maki, Phys. Rev. B **49**, 1397 (1994).
  - [20] Ch. Helm *et al.*, Phys. Rev. Lett. **89**, 57003 (2002).
  - [21] D. A. Ryndyk *et al.*, Phys. Rev. B **64**, 052508 (2001).

- [22] A. E. Koshelev and I. S. Aranson, Phys. Rev. Lett. **85**, 3938 (2000).